

Wave-Vector Conservation upon Hybridization of $4f$ and Valence-Band States Observed in Photoemission Spectra of a Ce Monolayer on W(110)

D. V. Vyalikh,^{1,*} Yu. Kucherenko,^{1,2} S. Danzenbacher,¹ Yu. S. Dedkov,¹ C. Laubschat,¹ and S. L. Molodtsov¹

¹*Institut für Festkörperphysik, Technische Universität Dresden, D-01062 Dresden, Germany*

²*Institute of Metal Physics, National Academy of Sciences of Ukraine, UA-03142 Kiev, Ukraine*

(Received 30 September 2005; published 19 January 2006)

Angle-resolved resonant photoemission data for a hexagonally ordered monolayer of Ce on W(110) are presented. The spectra reveal a splitting of the $4f^0$ ionization peak around a point in \mathbf{k} space where a degeneracy with a valence-band state is expected. The phenomenon is described within a simple approach to the periodic Anderson model. It is found that the Ce $4f$ state forms a band and hybridization predominantly occurs between the $4f$ and the valence-band states at the same wave vector.

DOI: [10.1103/PhysRevLett.96.026404](https://doi.org/10.1103/PhysRevLett.96.026404)

PACS numbers: 71.20.Eh, 79.60.Dp

The interaction of localized $4f$ states with itinerant conduction-band states leads to a series of correlation phenomena that have attracted considerable interest in the last few decades. Apart from spin-polarization effects that cause magnetic coupling via the RKKY interaction, hybridization may lead to noninteger f occupations, to heavy fermion behavior, or even to a breakdown of Fermi-liquid properties [1]. These effects are particularly strong at the beginning and the end of the rare-earth series as well as for Sm and Eu, where the energy differences between adjacent $4f^n$ configurations are relatively small as compared to magnetically ordered systems like Gd metal.

A typical and well studied system is Ce metal where hybridization of the trivalent $4f^1(5d6s)^3$ with $4f^0(5d6s)^4$ and $4f^2(5d6s)^2$ configurations is responsible for the isostructural α - γ phase transition related to a volume collapse of 15% and a quenching of the magnetic moment at low temperatures [2]. This hybridization is reflected in photoemission (PE) by a characteristic double-peaked structure of the $4f$ spectral function, where in addition to the ionization peak at around 2 eV binding energy (BE) expected for an unhybridized $4f^1$ ground state (“ $4f^0$ ” peak), a second feature appears at the Fermi energy (E_F) reflecting the Kondo-Suhl resonance with a final-state f occupancy close to 1. For the α phase the relative intensity of the latter with respect to the ionization peak is much larger as for the γ phase reflecting the increased hybridization of the ground state [3]. This effect may quantitatively be described in light of the Gunnarsson-Schönhammer approach [4] to the single-impurity Anderson model [5] (SIAM) that considers the interaction of an isolated $4f^1$ impurity at energy ϵ_f with surrounding valence-band (VB) states via hopping processes characterized by a hybridization parameter Δ . Consideration of $4f^2$ configurations is possible introducing the on-site Coulomb correlation energy U_{ff} . This approach allows us to relate electron spectroscopic data to results of low-energy experiments like specific heat, conductivity, and magnetization measurements and was successfully applied to many rare-earth systems [6]. A natural weakness of SIAM is, however, that it ignores

completely the effects of translation symmetry of structurally ordered solids. Consideration of the latter leads to the periodic Anderson model (PAM), for which, however, realistic theoretical approaches are still not available.

In PE such phenomena should be reflected by changes of the f signal as a function of a wave vector (\mathbf{k} vector), and, in fact, weak dispersion [7] and strong \mathbf{k} -dependent intensity variations of the Kondo resonance [8,9] have been observed in a few cases. Recently, respective effects in CePd₃ have been discussed [8] within a simple approach, which introduces a \mathbf{k} dependence considering the discrete energy distribution of VB states at each \mathbf{k} point as obtained from the band-structure calculation instead of a VB density of states obtained by integration over all \mathbf{k} points in the Brillouin zone. In light of this approach, large f hybridization is expected at points in \mathbf{k} space where valence bands approach the Fermi energy, and, in fact, good agreement between the observed intensity variations of the Kondo peak and properties of the band structure were obtained. This approach may be derived from PAM if the double occupation of the $4f$ states is ignored and \mathbf{k} conservation upon hybridization is assumed. Unfortunately, the latter is not trivial since due to the local character of the on-site Coulomb interactions the electron states with different \mathbf{k} may be coupled.

A possibility to check the validity of such an assumption is to study the behavior of the spectral function at points in \mathbf{k} space where the unhybridized f state is energetically degenerate with a VB state. Here, the model predicts a splitting of the ionization peak into two components corresponding to symmetric and antisymmetric linear combinations of the electron states. Respective effects are known from SIAM and lead, e.g., in angle-integrated PE spectra of Pr and Nd transition-metal compounds to huge splittings of the $4f$ PE signal [10,11]. In contrast to SIAM, however, the approach to PAM predicts such splittings to be restricted to the neighborhood of the \mathbf{k} points where degeneracy occurs. Ce transition-metal compounds, however, are not suitable candidates to demonstrate this effect, since the weak dispersion of the d bands leads to similar conditions at most

points of \mathbf{k} space, and different $4f$ binding energies at the surface and in the bulk lead to a further smearing out of the effect. An ideal candidate for such an experiment, however, is a Ce monolayer on W(110): As was shown by Gu *et al.* [12], Ce atoms form an ordered hexagonal overlayer on W(110) with interatomic distances shrinking continuously as Ce is added from 9% larger than that in γ -Ce to 3% smaller than that in the α phase. PE spectra reveal a respective increase of the Kondo-peak intensity with decreasing interatomic distances as expected for a γ - α transition. Since the overstructure is incommensurate and reveals a different symmetry as compared to the substrate surface (centered rectangular), only weak electron interactions with the substrate without a pronounced \mathbf{k} dependence are expected, and the spectra will be governed by the intrinsic properties of the two-dimensional Ce layer.

In the present contribution we show by means of angle-resolved resonant PE experiments at the Ce $4d \rightarrow 4f$ excitation threshold that the $4f$ -derived spectral function reveals a splitting of the ionization peak just around a point in \mathbf{k} space where a band of sd character crosses the BE position, ε_f , of the unhybridized $4f^1$ state. The data are analyzed within the mentioned approach to PAM [8], and excellent agreement between the theory and the experiment is obtained. The results show that, in fact, \mathbf{k} is conserved upon hybridization and confirms the validity of the respective assumption.

The experiments were performed at the Berliner Elektronenspeicherring für Synchrotronstrahlung using radiation from the U125/1-PGM-1 undulator. PE spectra were acquired with a VG CLAM-IV electron-energy analyzer. The overall-system energy resolution accounting for the thermal broadening was set to 150 meV (FWHM) and an angular resolution better than 1° was used. A structurally ordered monolayer of Ce metal was grown on a W(110) substrate kept at room temperature. Prior to the deposition of Ce, the W(110) substrate was carefully cleaned by repeated cycles of heating up to 1300°C in oxygen atmosphere for 15 min each (with a partial pressure of 5×10^{-8} mbar) and subsequent flashing at 2300°C . The samples prepared in this way exhibit a high crystalline quality as monitored by low-energy electron diffraction (LEED). The thickness of the deposited Ce was monitored with a calibrated quartz oscillator. All PE spectra were taken at $h\nu = 121$ eV, corresponding to the Ce $4d \rightarrow 4f$ resonance, where the electron emission from Ce $4f$ states considerably dominates over that from $5d$ states of tungsten that are close to a Cooper minimum of the photoionization cross section at this photon energy.

The lower panel in Fig. 1 shows PE spectra taken in normal emission geometry for two different surface densities of Ce atoms on the W(110) substrate. In both cases the corresponding LEED patterns indicate a hexagonal structure of the Ce layer. The spectrum denoted as A corresponds to the lowest Ce coverage where a hexagonal

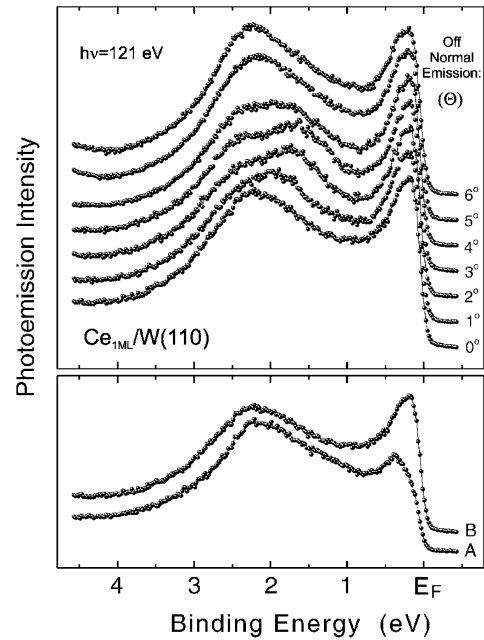


FIG. 1. Experimental on-resonance PE spectra of a Ce monolayer on a W(110) substrate taken at the Ce $4d \rightarrow 4f$ excitation threshold ($h\nu = 121$ eV). Lower panel: normal emission PE spectra obtained for different Ce coverages, γ -like Ce (A) and α -like Ce (B). Upper panel: angle-resolved PE spectra for α -like Ce taken along the $\bar{\Gamma}$ - \bar{K} direction of the surface Brillouin zone (Θ is the polar emission angle relative to the normal to the sample surface).

overstructure in the LEED pattern related to a respective arrangement of Ce atoms is still observed. The shape of this PE spectrum is typical for γ -like Ce (in this case the interatomic spacing is slightly larger than that in bulk γ -Ce). Further Ce deposition leads to decreasing spacings between Ce atoms, and the shape of the PE spectrum is changed to that of α -like Ce, with strongly enhanced intensity of the peak near E_F . The spectrum denoted as B corresponds to a Ce monolayer with interatomic spacing close to that of bulk α -Ce. To this point our results are in good agreement with those reported in Ref. [12].

The upper panel in Fig. 1 shows a set of angle-resolved PE spectra recorded along the $\bar{\Gamma}$ - \bar{K} direction of the surface Brillouin zone for the hexagonal α -Ce monolayer. One can see that the peak at E_F , indicating large hybridization of the system, remains practically unchanged in both intensity and line shape. However, the same is not true for the ionization peak. When going away from normal emission, it splits in, at least, two components. This energy splitting is maximal for polar emission angles between 2° and 3° . For polar angles larger than 5° this splitting disappears and the shape of the PE spectra shows no significant differences to the one of normal emission.

For interpretation of the obtained experimental data we consider first the valence-band structure of the hexagonal α -Ce(111) monolayer. Assuming that the incommensurate hexagonal Ce overlayer undergoes only weak interactions

with the W(110) substrate [12], we have calculated the electronic structure of a free atomic monolayer with interatomic distances of 3.42 Å that are equal to those in bulk α -Ce. Thereby, Ce atoms were substituted by La in order to suppress contributions of the 4*f* orbitals. The calculations were performed by the linear muffin-tin orbital method [13] using a supercell approach. A partial-wave expansion of the VB Bloch functions in the atomic spheres was performed up to $l_{\max} = 3$ in order to determine the VB components allowed for hybridization with the 4*f* orbitals according to the symmetry requirements.

The results of the calculations for the Γ -*K* direction are shown in the inset in Fig. 2. As follows from the geometry of our PE experiment, for an excitation energy of 121 eV the \bar{K} point is reached at a polar emission angle of 12.6°. Thus, the \mathbf{k} points in the given symmetry direction could be characterized by respective polar angles. The bottom of the VB is found at the Γ point at a BE of 2.4 eV (with respect to E_F). The respective Bloch wave function reveals mainly *s* and *d* character: 62% and 34%, respectively. Contributions of *p* and *f* character are negligible. About 4% of the charge density is distributed outside the La atomic spheres. When going away from the Γ point (off normal emission) the valence band shows a parabolic dispersion, and its angular momentum character becomes smoothly changed. At a \mathbf{k} point that corresponds to the 5° emission angle the *s* component decreases to 38%, the *d* component slightly increases to 38%, and *p* and *f* states contribute by 12% and 8.5%, respectively. Other energy bands are close to E_F and have a strong *d* character (about

60%) but also significant *f* contribution (up to 20%). The *f* contribution is derived from tails of *p* and *d* orbitals of surrounding atoms, which are reexpanded by partial waves around the new center.

The energy position of the unhybridized 4*f* level in Ce metal is about 1.5 eV [14]. Therefore, assuming the 4*f* states to create a dispersionless band at this energy, this *f* band should cross the parabolic VB close to a \mathbf{k} point corresponding to 3°. In the region of this point hybridization effects between 4*f* and VB states are expected. The starting point of our analysis, how these effects influence the 4*f* emission, is the approach based on a simplified PAM applied recently to CePd₃ [8].

We consider the Anderson Hamiltonian:

$$\begin{aligned} H = & \sum_{\mathbf{k},\sigma} \varepsilon(\mathbf{k}) d_{\mathbf{k}\sigma}^\dagger d_{\mathbf{k}\sigma} + \sum_{\mathbf{k},\sigma} \varepsilon_f(\mathbf{k}) f_{\mathbf{k}\sigma}^\dagger f_{\mathbf{k}\sigma} \\ & + \sum_{\mathbf{k},\sigma} V_{\mathbf{k}}(\varepsilon) (d_{\mathbf{k}\sigma}^\dagger f_{\mathbf{k}\sigma} + f_{\mathbf{k}\sigma}^\dagger d_{\mathbf{k}\sigma}) + \frac{U_{ff}}{2} \sum_{i,\sigma} n_{i,\sigma}^f n_{i,-\sigma}^f \\ = & \sum_{\mathbf{k}} h_0(\mathbf{k}) + u, \end{aligned} \quad (1)$$

where the VB states $|\mathbf{k}\sigma\rangle$ have a dispersion $\varepsilon(\mathbf{k})$ and are described by creation (annihilation) operators $d_{\mathbf{k}\sigma}^\dagger$ ($d_{\mathbf{k}\sigma}$). The operator $f_{\mathbf{k}\sigma}^\dagger$ creates an *f* electron with momentum \mathbf{k} , spin σ , and energy $\varepsilon_f(\mathbf{k})$. We assume that a nonhybridized *f* band has no dispersion: $\varepsilon_f(\mathbf{k}) = \varepsilon_f$. The two electron subsystems (VB and *f* states) are coupled via a hybridization $V_{\mathbf{k}}(\varepsilon)$, and finally U_{ff} is the Coulomb repulsion between two *f* electrons localized on the same lattice site.

The main problem to treat the PAM is due to the term describing the local Coulomb interaction U_{ff} . The transformation of this term to a \mathbf{k} representation leads to a mixing of states with different \mathbf{k} values, which makes the problem difficult to handle quantitatively. Neglecting weak contributions of 4*f*² configurations to the initial and final-state configurations results in \mathbf{k} conservation and allows us to diagonalize the Hamiltonian for each particular \mathbf{k} point of the surface Brillouin zone. This approximation corresponds to $U_{ff} \rightarrow \infty$.

For the \mathbf{k} -dependent hybridization matrix element $V_{\mathbf{k}}(\varepsilon)$ we use the calculated respective *f*-projected local expansion coefficients $c_f(E, \mathbf{k})$ of the Bloch functions around the rare-earth sites:

$$V_{\mathbf{k}}(E) = \Delta [c_f(E, \mathbf{k}) + b(E)], \quad (2)$$

where Δ (like ε_f) is a constant, adjustable parameter. In order to take into account the influence of the W(110) substrate we have introduced into the hybridization matrix element also a smooth parabolic function $b(E)$ that starts at 4 eV BE and slowly increases to E_F . It describes the electron-charge density of W atoms outside the uppermost W layer. Because of the incommensurate Ce overlayer, this charge density is seen by the average Ce atom as a weak smooth background. The integral contribution of $b(E)$ to

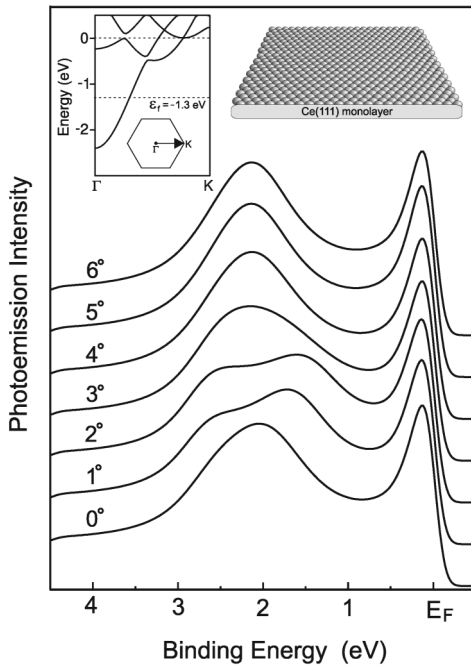


FIG. 2. Calculated PE spectra of an α -Ce(111) monolayer for different emission angles (given in the figure). Inset: the energy-band structure for the Γ -*K* direction.

the hybridization function does not exceed 10%. It has no qualitative effect on the shape of the calculated PE spectra but increases the linewidths in agreement with the experiment.

Diagonalizing the Hamiltonian matrix for the initial and final (electron-removal) states, we can calculate the spectral function for the $4f$ emission. This stage to solve the simplified PAM problem is formally similar to the one encountered in SIAM (as described in detail in Ref. [15]) with the difference, however, that now the shape of PE spectra is changed as a function of \mathbf{k} . A series of calculated spectral functions is shown in Fig. 2 for the same direction in \mathbf{k} space, for which the experimental data in Fig. 1 were taken. The spectral functions were obtained using the parameters $\varepsilon_f = -1.3$ eV and $\Delta = 0.9$ eV. These parameters deviate by about 10% from those obtained from an analysis of the bulk $4f$ spectra of α -Ce in the framework of SIAM [14] due to the neglecting of $4f^2$ admixtures and the different distribution of VB states applied. Note that ε_f and Δ represent the only free adjustable parameters of the fit and are fully determined from the simulation of one particular PE spectrum. An energy-dependent lifetime broadening parameter of the form $\Gamma_L = 0.03$ eV + $0.09E$ was used, where E denotes the BE with respect to E_F . The calculated spectral functions were additionally broadened with a Gaussian ($\Gamma_G = 0.08$ eV) to simulate finite instrumental resolution and an integral background was added to take into account inelastic scattering events.

The calculated PE spectra change their shape with an increase of the emission angle. The ionization peak is split into two maxima that diverge from each other by up to about 1 eV. This behavior is in excellent agreement with that observed in the experimental PE spectra. Thus, the splitting of the peak at 2 eV BE in the angle-resolved spectra of the Ce monolayer on the W(110) may be ascribed to the interaction of the $4f$ states with the parabolic VB that leads to the typical picture of two hybridized energy bands.

Our calculations show that in the system of γ -like Ce atoms (a hexagonal monolayer with larger interatomic distances) the dispersion of the valence bands is similar to that of α -like Ce atoms discussed above. In the γ -like Ce layer the bottom of the VB is, however, shifted downward in energy (to 2.7 eV) and reveals more s character while less d character (67% and 26%, respectively). The d character of the bands near E_F (over 70%) is stronger than in the α phase. This indicates decreasing of s - d mixing in the chemical bonding, or, in other words, less bonding contributions of d states. With increasing interatomic distance the f part of the Bloch-function expansion in the Ce sphere also decreases leading to decreased hybridization strength.

Nevertheless, in the γ -like Ce monolayer the $4f$ band will also cross the parabolic VB. Thus, similar hybridization effects should exist, although the splitting in the PE spectra will be smaller due to the reduced hybridization strength. In order to observe these effects experimentally also for γ -like Ce, PE spectra with higher resolution should be recorded. We believe that finite energy and angular resolutions were the reason why the described hybridization effects were not observed earlier by the authors of Ref. [12].

In conclusion, we have shown that \mathbf{k} -dependent splittings of the $4f$ ionization peak of Ce/W(110) are correctly described in the framework of the simplified periodic Anderson model. Our results show that the wave vector is conserved upon hybridization.

This work was supported by the Deutsche Forschungsgemeinschaft, SFB 463, Projects TP B4 and TP B16 and BMBF Project No. 05-SF8OD1/4. We are grateful to R. Follath for the expert operation of the U125/1-PGM-1 undulator beam line.

*Corresponding author.

Electronic address: vyalikh@physik.phy.tu-dresden.de

- [1] P. Fulde, *Electron Correlations in Molecules and Solids* (Springer, Heidelberg, 1995); P. Wachter, *Intermediate Valence and Heavy Fermions*, edited by K. A. Gschneider *et al.*, Handbook on the Physics and Chemistry of Rare Earths Vol. 19 (Elsevier Science, Amsterdam, 1994); L. Degiorgi, *Rev. Mod. Phys.* **71**, 687 (1999).
- [2] D. C. Koskenmaki and K. A. Gschneider, in *Handbook on the Physics and Chemistry of Rare Earths*, edited by K. A. Gschneider and L. Eyring (Elsevier Science, Amsterdam, 1978), Vol. 1, p. 337.
- [3] D. Wieliczka *et al.*, *Phys. Rev. B* **26**, R7056 (1982).
- [4] O. Gunnarsson and K. Schönhammer, *Phys. Rev. Lett.* **50**, 604 (1983); *Phys. Rev. B* **28**, 4315 (1983).
- [5] P. W. Anderson, *Phys. Rev.* **124**, 41 (1961).
- [6] J. W. Allen *et al.*, *Adv. Phys.* **35**, 275 (1986).
- [7] A. B. Andrews *et al.*, *Phys. Rev. B* **53**, 3317 (1996); S. L. Molodtsov *et al.*, *ibid.* **57**, 13 241 (1998).
- [8] S. Danzenbächer *et al.*, *Phys. Rev. B* **72**, 033104 (2005).
- [9] A. B. Andrews *et al.*, *Phys. Rev. B* **51**, 3277 (1995); M. Garnier *et al.*, *Phys. Rev. B* **56**, R11399 (1997); **58**, 3515 (1998).
- [10] Yu. Kucherenko *et al.*, *Phys. Rev. B* **65**, 165119 (2002).
- [11] Yu. Kucherenko *et al.*, *Phys. Rev. B* **66**, 165438 (2002).
- [12] C. Gu *et al.*, *Phys. Rev. Lett.* **67**, 1622 (1991).
- [13] O. K. Andersen, *Phys. Rev. B* **12**, 3060 (1975).
- [14] Yu. Kucherenko *et al.*, *Phys. Rev. B* **66**, 155116 (2002).
- [15] R. Hayn *et al.*, *Phys. Rev. B* **64**, 115106 (2001).